



THE 21st CHESAPEAKE SAILING YACHT SYMPOSIUM
ANNAPOLIS, MARYLAND, MARCH 2013

The Evolution of Design: SALTS' New Sail Training Schooner Project

Stephen Duff, Dept. of Architecture, University of Oregon; SALTS Sail and Life Training Society

Fabio Fossati, Department of Mechanics, Politecnico di Milano, Milano – Italy

Andy Cloughton, Wolfson Unit MTIA, University of Southampton, Southampton – England

William Krzymowski, SALTS Sail and Life Training Society, Victoria, BC – Canada

Tony Anderson, SALTS Sail and Life Training Society, Victoria, BC – Canada



1:15 scale model of SALTS' new schooner in the Politecnico di Milano boundary layer wind tunnel
(Sail plan S4 at 60° AWA)

ABSTRACT

The Sail and Life Training Society is building a new purpose-designed 35m wooden sail-training schooner for unrestricted foreign-going operations. Working with an international team of consultants, SALTS has initiated an ambitious agenda of analytical and experimental investigations to support design, including a parametric study of hull form as it relates to stability at high angles of heel, the development of bespoke parametric design and analysis tools using the graphical algorithm editor Grasshopper, a towing tank campaign at the Wolfson Unit to investigate the behavior of three keel profiles, and a wind tunnel campaign at Politecnico di Milano to investigate the behavior of fifteen sail plans. Preliminary results from these studies will be presented, set in the context of the unfolding story of the evolution of the design of the new vessel.

NOTATION

AWA	Apparent wind angle
CE	Centre of effort
C_{ea}	Centre of effort longitudinal position
C_{eh}	Centre of effort height
C_D	Drag coefficient
CG	Centre of gravity
C_L	Lift coefficient
CLR	Centre of lateral resistance
C_{rr}	Residuary resistance coefficient
C_x	Driving force coefficient
C_y	Heeling force coefficient
Fn	Froude number
F_x	Driving force
F_y	Heeling force
GZ	Righting arm
Gz_j'	Righting arm of transverse plane 'i'
HA_1	Wind (gust) heeling lever arm at 0° heel
HA_2	Mean wind heeling arm at any heel angle φ
H_{Agust}	Wind (gust) heeling arm at any heel angle φ
H_{eff}	Effective height
LSA	Life saving appliances
R	Resistance
RM	Righting moment
R_r	Residuary resistance
S	Sail area
SF	Side force
SPS	Code of Safety for Special Purpose Ships
T_{eff}	Effective draft
V	Speed
v	Wind speed
V_a	Apparent wind speed
VCG	Vertical centre of gravity
VPP	Velocity Prediction Program
Δ	Displacement
ρ_a	Density of air
ρ_w	Density of water
φ	Heel angle

INTRODUCTION

The Sail and Life Training Society (SALTS) is a registered Canadian charitable organization based in Victoria, BC, that has been taking young people to sea in traditional wooden sailing vessels since 1974. With program demand far exceeding existing capacity, and drawing on the experience of four major construction projects and over 300,000 nautical miles of sailing, SALTS has set out to build a new purpose-designed, deep-sea sail-training vessel. The new wooden boat will be rigged as a two-masted square topsail schooner, and has a current design displacement of 229 tonnes, length overall of 35m and sparred length of about 43m. While the design and character of the new vessel are rooted in the traditions of historical workboats, the new schooner will be built to meet rigorous safety and function-driven design criteria.

In support of the design process, SALTS is working with an international team of consultants to bring their

expertise to bear on critical aspects of the design. An ambitious agenda of experimental and analytical campaigns is now underway, aiming to inform particulars of design, while more broadly contributing to the body of knowledge pertaining to vessels of this class.

This paper presents an overview of the project, principal design issues, details of the major research programs, preliminary results, and the scope of future work being initiated or planned. Although the schooner described herein might be considered old school, the technical approach is absolutely relevant to any sailing vessel that must be designed to meet an operational draft limitation and in compliance with a modern regulatory regime.

PROJECT ORIGINS

Since its founding, SALTS' custom has been to build and sail conversions or replicas of traditional wooden workboats, such as the society's current schooners the *Pacific Swift* and the *Pacific Grace*. When the new vessel was first conceived, initial discussions focused on what type of vessel to build. It was decided that the starting point for design would be North Sea Pilot Schooners—boats with a reputation for sea-worthiness that kept station offshore to transfer pilots to incoming ships (Figure 1), made famous in the sail-training world by the voyages of Irving Johnson aboard his schooners *Yankee*.



Figure 1 – Elbe pilot schooner *Cuxhaven*, c. 1890

Early on, however, we decided that rather than building a replica of an historical precedent, a new design would be developed along the lines of the class, but tailored to meet SALTS' particular needs. Paul Gartside, naval architect for the *Pacific Grace*, was commissioned to produce four preliminary design studies (the first shown in Figure 2). The general arrangement matched that of SALTS' existing schooners, with two accommodation compartments for trainees forward, and an integrated navigation station and crew cabin aft. As work proceeded with the increasing involvement of the first author, initial design criteria were defined, the general hull form evolved (larger, with a plumb stem), Gartside refined the lines by hand, and the

general arrangement was worked over in detail.

This period marked the start of a transition to an explicit intention to build a purpose-designed boat, increasingly less-related to the original North Sea precedents. It also marked the beginning of the definition of clearly identified design and performance criteria.

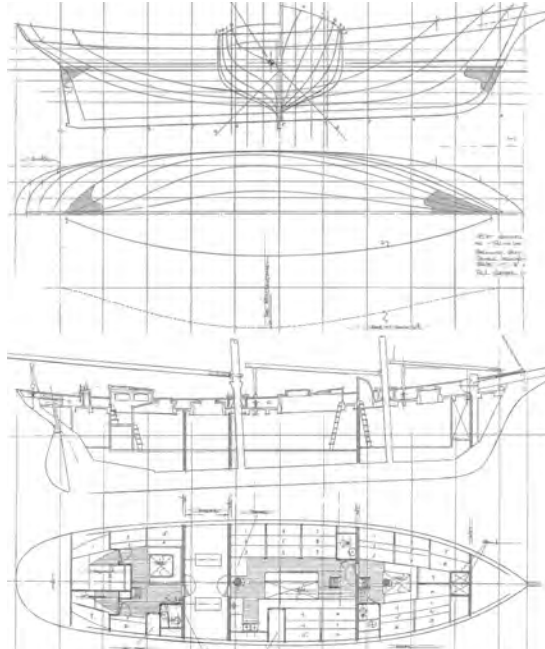


Figure 2 – First design study (Gartside, 2007)

GENERAL DESIGN OBJECTIVES

SALTS’ mission is to take young people to sea on character-building trips of five to ten days duration off the coast of British Columbia, and on longer deep-sea voyages to international destinations. The new boat will serve both programs, but it is being designed specifically for offshore sailing.

With SALTS’ existing boats as reference, general design objectives include increasing the separation of spaces belowdecks to increase safety and efficiency, enhancing the livability of crew quarters, improving ship-wide storage systems, and refining numerous details of layout.

SAFETY

Foremost among the design criteria—and central to all aspects of the project—is safety. At times, the new boat will sail with children; at other times it will be far offshore: while we would like to make a beautiful boat that sails well, safety is the first priority in design. In light of various 20th and 21st century sail-training casualties (Curry 2010; Parrott 2003; Transportation Safety Board of Canada 2011). SALTS has established rigorous design goals for stability, deck safety, sea keeping, and emergency preparedness.

A pivotal moment in the evolution of the design of the new boat was a meeting held between two of the authors and Bill Curry, Captain of the *Concordia* when it was knocked down and lost in 2010, and Sugar Flanagan, first

mate on the *Pride of Baltimore* when that vessel capsized and sank in 1986. Both were exceedingly generous with their time and recollections. Detailed review of those incidents, and the collective scrutiny of SALTS’ intentions, criteria, and preliminary designs, led to significant changes in design attitudes, objectives, and outcomes.

Stability

In the early stages of design, Paul Gartside remarked to the first author that the design of this boat should be first and foremost about stability—words that have remained a touchstone throughout the ensuing work.

Canadian stability regulations for sail training vessels follow the MCA standards developed at the Wolfson Unit over 20 years ago (Deakin 1991, 2009). Like other national standards, one defining characteristic is the requirement of a minimum range of positive stability of 90°. A GZ curve that meets that standard is shown in Figure 3.

While the 90° requirement was adopted as ‘being realistically achievable for seagoing vessels’ (Deakin 2011), it is based on the assumption that the wind has no vertical component. If such were the case, however, the wind heeling arm curve (HA_{gust}) would shift to the right to the same degree as the angle of inclination of the wind (see the Endnote for a brief explanation of the derivation and use of the MCA heeling arms and maximum steady heel angle). It can be seen that for the illustrated GZ curve, due to the similarity in slopes of the two curves, only a small shift in the HA_{gust} curve will result in a failure to reach a static equilibrium condition (the GZ and HA_{gust} curves will not intersect) and the vessel will be knocked down. If the angle of inclination of a strong gust is high, it is reasonable to assume that if enough sail is set—barring a rig failure—most any sailing vessel will be knocked down.

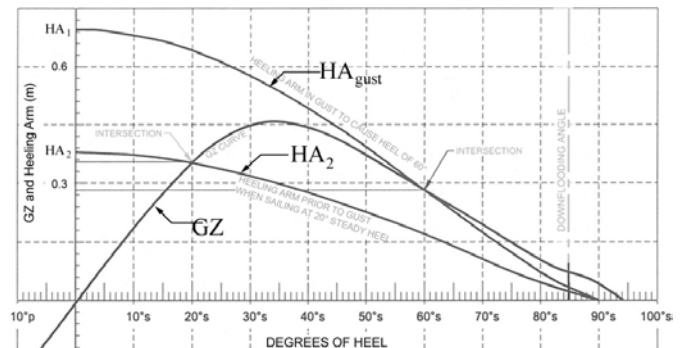


Figure 3 – A minimally compliant GZ curve

Moreover, if the GZ curve of a vessel only just meets the 90° requirement, as in Figure 3, the instantaneously available righting moment when a vessel is on its beam-ends will be minimal. As Deakin points out (*ibid*), it is difficult to quantify the extra energy needed to pull the sails up out of the water. Further recognizing that a vessel’s stability condition may rapidly deteriorate due to downflooding, a boat with a minimally compliant stability curve, once knocked down, may be down for good.

Fundamental to the design of SALTS' new schooner are self-imposed stability criteria that significantly exceed effective Canadian and international standards for sail training vessels. Of particular concern is the response of the vessel to high-energy short-term wind events—gusts and squalls, particularly those with vertical wind components—and its righting moment at extreme angles of heel. SALTS intends to build a stiff vessel with a large difference in the slopes of the GZ and *HAgust* curves, and with significant reserves of righting energy well past the operational maximum steady angle of heel (at the intersection of the GZ and *HA*₂ curves), including in a complete knockdown condition. Design strategies include a very large external ballast keel, the use of hollow spars, careful attention to weight distribution, and optimization of hull form as it relates to vessel stability.

Deck Safety

Another area of significant concern is deck safety. While open decks are prime living spaces, they are also parts of working machines, and can expose the crew to life-threatening conditions. It is only six years since a Canadian crewmember was fatally lost overboard from the *Picton Castle*.

For SALTS' new vessel, bulwark and lifeline heights will be raised, arrangements of running lifelines for safety harnesses will be carefully designed, visibility from the control station to the deck will be improved, and extra attention will be paid to the run of lines and the layout of gear.

Evacuation, Abandon Ship, and Knockdown

In the aforementioned meeting with Curry and Flanagan, a subject that we examined closely was the turn of events after the knockdowns. In those and other incidents, people have been trapped below, trapped behind jammed doors, trapped on top of inward-opening doors by their own weight, fallen the breadth of the ship once it was on its side, had difficulty climbing to openings to the deck, and been unable to access life saving appliances for a variety of reasons.

The heightened awareness that arose from that discussion brought all aspects of the design under scrutiny and led to design responses to as many emergency scenarios as we could imagine. These include the improvement of emergency egress routes; attention to the direction of door swings; the provision of knock-out panels in partition doors; consideration of egress routes at extreme angles of heel; the provision of climbing holds on the deck-head and bulkheads—anticipating a 90° change in orientation; and the careful distribution and positioning of life saving appliances (LSA).

The distribution of LSA on deck merits special attention. We realized that in the event of a sustained knockdown, if the LSA were distributed around the perimeter of the deck—as might be thought optimal—many would be inaccessible. The width of this boat is such that on the submerged side, the depth of LSA containers

might not be sufficient to trigger their hydrostatic releases, but they would be too deep for all but the most determined attempts at access. Many of the LSA on the exposed side would also be inaccessible, as the vertical distance between the centerline deck structures and the LSA containers would put them beyond reach, except by the extraordinary measure of climbing up on the outside of the hull and somehow reaching over the bulwark to remove the gear, without dropping a potentially harmful container lid on someone in the water below. Figure 4 shows a comparison of a possible layout of LSA around the deck perimeter, with that of a scheme with most LSA positioned along the centerline. In the latter, note also the increased dispersal of LSA, which we deem will decrease the probability of denied access due to unforeseen events in an emergency.

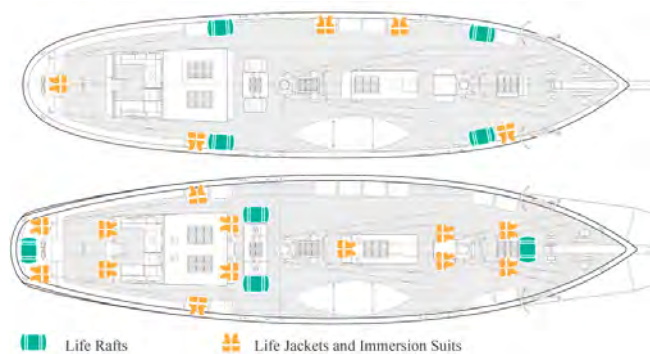


Figure 4 – Possible distribution of life-saving appliances

Rig Reliability

In recent years, the schooner *Zodiac* was dismantled, the brig *Fryderyk Chopin* suffered a major failure of both masts, and the *Pride of Baltimore II* experienced a catastrophic rig collapse. All are sail training vessels.

Although we are only in the early stages of rig design and detailed discussion would be premature, rig reliability is being taken very seriously, and the analysis and design process will be rigorous. Of particular concern are the design of masts, spars and critical elements of rig hardware (two of the above failures were attributed to hardware failure) and wherever possible, the provision of structural redundancy.

PRELIMINARY DESIGN

Once preliminary design started in earnest, the principal design effort was established in-house, based at the University of Oregon and in SALTS' shipyard attic. A strength of this project is the fact that the principal designers are their own clients, bringing to the task an intimate understanding of SALTS' needs based on decades of experience sailing with the society.

Early design work was done entirely in pencil, but with the involvement of a group of dedicated students at the University of Oregon, and then the addition of author William Krzymowski to the design team, the design process evolved from drawing by hand (that media will always be important) to one increasingly digital.

Rig and Sail Plan

Preliminary design of the rig and sail plan also involved the analysis of precedents, and was influenced by years of sailing experience at SALTS. Given the age and inexperience of the trainees who will work the boat, limits on the size of the mainsail and jibs were imposed, and certain rig details were fixed. The main boom on the *Pacific Grace* is nearly 19m long: during deep rolls in large seas, it forcefully plunges into the sea, jarring the entire rig (Figure 8). Early on, we decided to significantly shorten the boom to avoid this, even though the new boat would be larger than the *Pacific Grace*. This was consistent, however, with a goal to increase the overall aspect ratio of the rig, and the mainsail in particular.



Figure 8 – Boom immersion on the *Pacific Grace*, with reefed main (left); Split courses on the *Pacific Swift* (right)

The square topsail rig was chosen before we began, as it works brilliantly for SALTS. The flexibility of the sail plan supports the wide range of sailing conditions the new boat will encounter. Climbing out on yards, furling square sails and pulling on braces enhance the sail-training mission.

For downwind sailing, we can fully dress the foremast with square sails by setting split courses on jackstays forward of the mast (Figure 8). Purists may scoff at these uncommon sails, but they can be safely set from the deck and struck very quickly without sending trainees aloft; they eliminate the stability-degrading weight of additional yards, were the boat rigged as a brigantine; and they do not conflict with a foresail raised on hoops. They also afford useful, if unusual, sail combinations: windward course, foresail, and square topsail set with the mainsail can be a powerful combination on a broad reach.

Initial comparison of sail-area to displacement and sail-area to wetted-surface ratios with known precedents gave rise to a concern that the boat might be underpowered in light airs, but we have adjusted sail areas to a point we think is viable. For downwind sailing, we will also carry a triangular raffle to set above the upper yard, and we aim to rig a large fisherman staysail. The latter is unusual and difficult to rig in combination with the square topsail, as the braces intersect the plane of the sail. By decreasing the chord length of the sail (and increasing its aspect ratio), running braces out to spreaders and shrouds, and possibly

fitting brace tricing lines, the combination is workable, as we determined through 3d design studies and later confirmed when we built the wind tunnel model.



Figure 9 – Preliminary sail plan (2010-2011)

Initially, helm balance was addressed by considering the lead between geometric centroids of the sail plan and underwater hull profile, although the limitations of this approach were well understood.

The rig evolved through several preliminary iterations, one of which was drawn up for presentation and fundraising purposes (Figure 9). At that time, the masts had significant but not severe rake. The mainsail had an aspect ratio higher than that found on large traditional schooners like the *Pacific Grace*. Aesthetically, however, the overall impression of this sail plan is unsatisfactory. This is largely attributable to the angle of the leeches of the mainsail and foresail, and the combination of proportions and geometries of individual sails not working well together.

THE OPEN SEA PROJECT™ Grasshopper and Rhinoceros

To solve various analysis problems and to increase efficiency in design, two of the authors have been developing a suite of parametric analysis and design tools using the graphical algorithm editor *Grasshopper*, a plug-in for the NURBS surface modeling program *Rhinoceros*.

The principal user interface in *Grasshopper* is a node-based editor. *Scripts* are created by dragging *components* and *parameters* from *palettes* onto a *canvas* and connecting inputs and outputs to create program algorithms. Components may generate, manipulate, or measure *Rhino* geometry; or they may contain numeric, textual, audio-visual, or other functions. *Sliders* can be introduced to control functions or settings, and data can be exported. Figure 10 shows part of a *Grasshopper* script developed for this project that generates a curve of displacements for a hull surface in *Rhino* and finds the correctly trimmed flotation plane for a specified angle of heel.

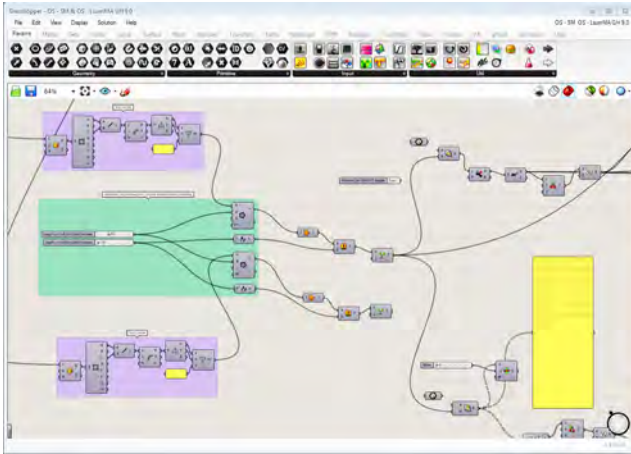


Figure 10 – An *Open Sea* script in *Grasshopper*.

Project Description and *Open Sea* Tools

As our design process evolved, we increasingly used *Grasshopper* tools to the point where now, *Rhino* models and linked parametric algorithms constitute the principal design environment. A growing library of task-specific algorithms has led to the definition of the *Open Sea Project*TM, an intended on-line nexus for the development and exchange of open-source *Grasshopper*-based algorithmic routines for naval architecture.

To date, *Open Sea* analysis and design tools include routines for the comprehensive hydrostatic analysis of hull models; hull-form visualization and analysis; weight and centre of gravity analysis and tracking; intact stability studies; interactive hull structure and rig geometry generation; preliminary sail shape modeling; and the interference analysis of structure, general arrangement, and ship systems.

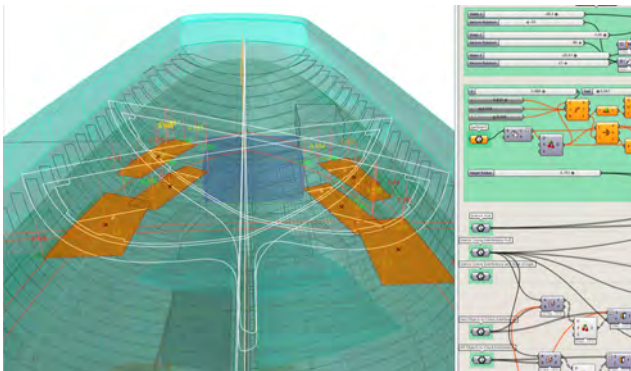


Figure 11 – *Open Sea* interference analysis.

Figure 11 shows the interior of a *Rhino* hull surface with a *Grasshopper* script used to examine berth dimensions and overhead clearances, to ensure that regulatory requirements and SALTS design criteria are satisfied. Frame profiles generated by *Open Sea* can be seen, along with tanks and the volume of a critical service space.

In Figure 12, the *Grasshopper* script measures spar volumes, locates and assigns an ID number to their

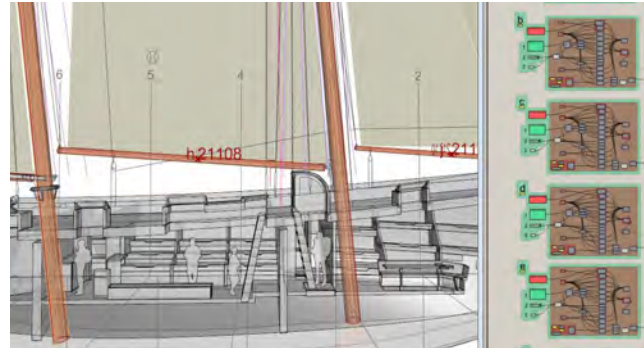


Figure 12 – *Open Sea* weight and CG analysis.

centroids, and saves the data to a spreadsheet. This application is similarly used for all weight data, and with data exported to *Excel*, serves as the principal weight and CG management system for the project. It is interactive, and data can be updated as design models evolve.

Further details of the *Open Sea* project will be presented in a future publication.

PARAMETRIC STABILITY ANALYSIS

Precedent Curves

During preliminary design, two of the SALTS authors started running intact stability analyses on a series of preliminary hull models using GHS software. With an assumed VCG of 0.0m (referencing the waterline), we compared stability data from a hull variant (#4f) with data

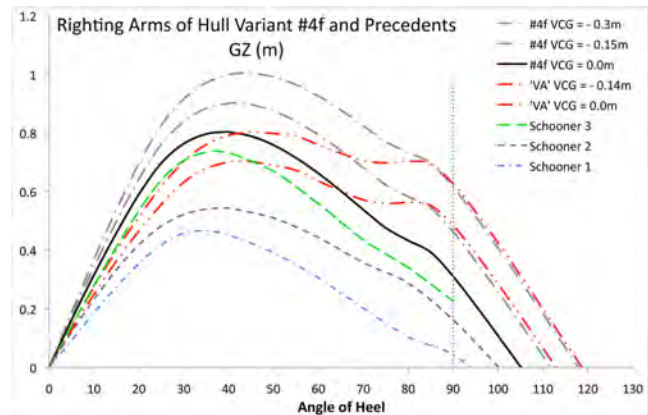


Figure 13 – Righting arms of #4f and precedents

from three existing vessels (*Schooners 1* and *2*, both with internal ballast only; and *Schooner 3*, with internal and 20 tons external ballast). #4f has a GZ curve somewhat better than that of *Schooner 3* and significantly better than *Schooners 1* and *2* (Figure 13), but there is a 61% drop in the value of GZ from GZ_{max} at $\sim 39^\circ$ to 90° .

At that time we obtained the stability curve for an American schooner (44 tons external ballast) that exhibited a very shallow mean slope between GZ_{max} and $\sim 85^\circ$. To examine why, we built a comparable model (called 'VA') in *Rhino* that exhibited similar stability behavior to the original. Like the original, 'VA' has high freeboard, long

overhangs and relatively narrow beam. Reserve buoyancy is 189% of displacement (cf. 152% in #4f and 130% in *Schooner 1*). Two dashed red GZ curves for 'VA' can be seen in Figure 13: the lower one has the same VCG as #4f (0.0), while the upper one matches GZ_{max} with a VCG of -0.14m. If the goal is to maintain significant reserves of righting energy at extreme angles of heel, shallow descending slopes of the GZ curve at heel angles greater than GZ_{max} —like those exhibited by 'VA'—would be very beneficial, other principal stability parameters being equal.

Beam and Freeboard Hull Matrix

To quantify the relationship between hull form and the shape of the curve for the purpose of making design decisions, we modified the geometry of various *Rhino* models and ran them in GHS. An early study aimed to quantify the effect of incremental changes to beam and freeboard of the prototype hull. Figure 14 shows a section through a matrix of 32 hulls that were generated in *Rhino*. The parent hull is black; red derivatives were generated in 30cm increments of beam and 10cm increments of freeboard.

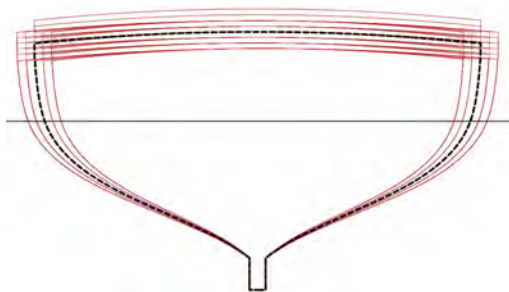


Figure 14 – Matrix of transverse sections

Figures 15 and 16 show GZ curves for two series of beam and freeboard variations. The curve for the parent hull is shown as the solid black line and the matching curve for 'VA' is shown in red for reference. While the results are in no way new, they do quantify cause and effect.

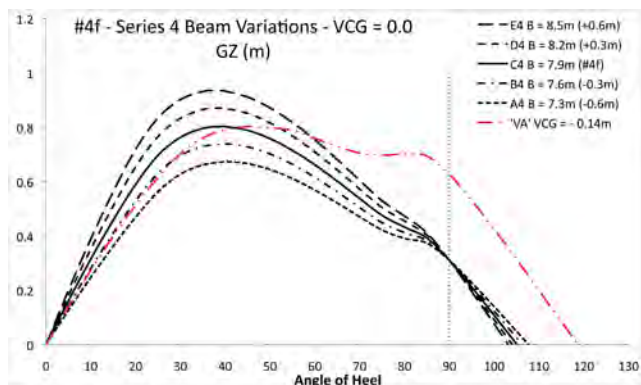


Figure 15 - #4f with five variations of beam

As expected, increasing beam increases GM and GZ_{max} , but it increases the downward slope of the curve past the angle of GZ_{max} and has little effect on righting moment at

extreme angles of heel. Reducing beam certainly reduces the slope of the latter part of the curve, but it is counter-productive in terms of GM, GZ_{max} and area under the curve. The shallow slope is consistent with the known behavior of vessels with low beam to depth ratios, and partly explains 'VA's curve.

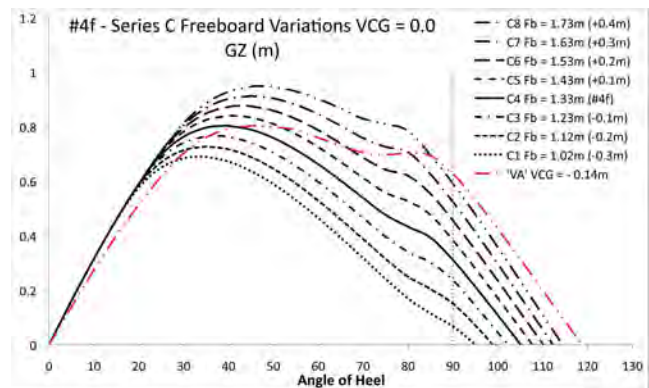


Figure 16 - #4f with eight variations of freeboard

Increasing freeboard changes nothing, of course, until the point of (the control's) deck-edge immersion is reached, after which it is beneficial. Note, however, that the downward slope of the curve is decreasing only slightly, not nearly enough to produce a curve like those seen in Figure 13 (reserve buoyancy of the upper black curve in Figure 16 is 190%, matching that of 'VA'). High reserve buoyancy, while beneficial, does not solely account for the shallow curves of 'VA'.

Parametric Hull Geometry Analysis

To further quantify cause and effect, we looked at other physical changes. Figure 17 shows #4f and 'VA' with their overhangs cut off. Figure 18 shows #4f and 'VA' with their deck sheer cut off tangent to its lowest point (original deck edges outlined for reference).

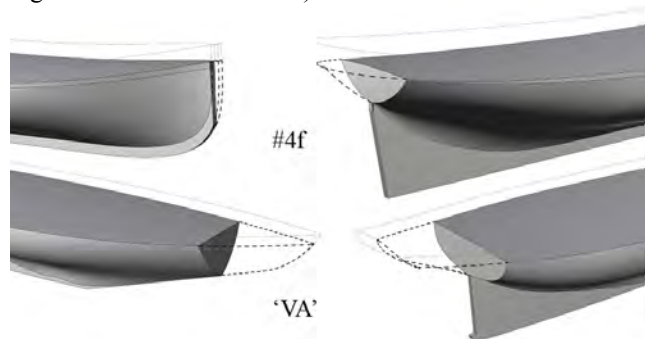


Figure 17 – Overhangs removed for analysis

The GZ curves for these studies can be seen in Figure 19. The effect of the overhangs in #4f is negligible, but for 'VA', is significant. The sizable volume of the overhangs in 'VA' (8.7% of total reserve buoyancy; cf. 1.4% in #4f) contribute to the effective flattening of the slope, but there is still a large delta between the curves for 'VA' without overhangs and the #4f curve below.

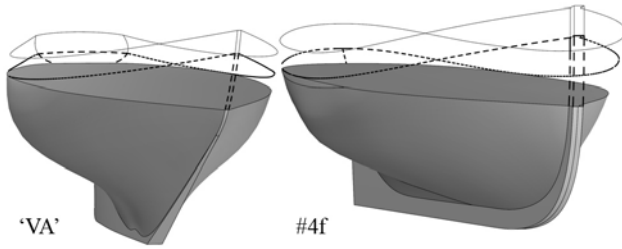


Figure 18 – Deck shear removed for analysis

The effect of the volume of the deck shear is also significant, and it is consistent with the effect of changes in freeboard seen in Figure 16.

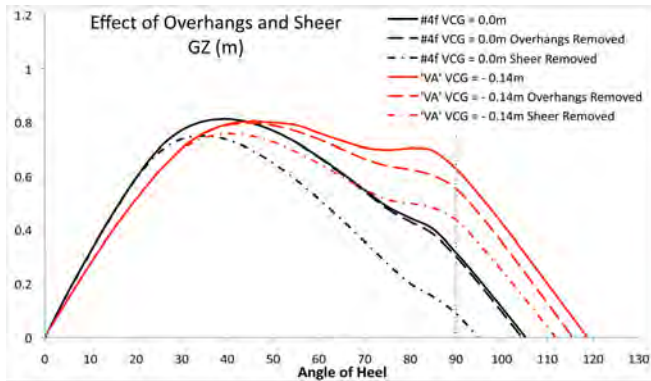


Figure 19 – Removal of overhangs and shear

These studies did not reveal insights new to naval architecture. They were intended to help us design the boat, and we also quantified the effects of deck camber, flare, tumblehome, and different degrees of hollowness in the garboards below the waterline; aiming to build up a comprehensive and quantitatively understood picture of the implications on stability of design decisions regarding hull form geometry for this type and size of hull.

Open Sea FARE

Fully understanding the shallow descent of the GZ curve in question remained elusive. To penetrate the issue more deeply, we built an *Open Sea* tool we call FARE (Form Analysis of Righting Energy). The central question is where, in a progressively heeling hull volume, is the sustained net positive righting buoyancy coming from?

We realized we could evaluate this if we could slice the hull volume transversely and longitudinally into a matrix of vertical prismatic volumes, and then evaluate the individual contributions of each prism to righting moment throughout the entire arc of heel. *Grasshopper* is the ideal tool for this, as it is simply a matter of manipulating and measuring geometry. With limited space in this paper, we present a synopsis of parts of the *Open Sea* routine.

Figure 20 shows transverse sections of two hulls: 'VA' and '#4f'. For the sake of argument we will consider the purple-coloured figure, a section through 'VA'. Note that we are looking at sections cut through 3d *Rhino* models of the two hull envelopes: the model surfaces are invisible and

only the section cuts can be seen.

The centroids of the transverse sections are shown by the symbols 'X'. A given sections' local moment arm is defined as Gz_j . The centres of buoyancy (CB) and centres of gravity (CG) of the 3d hulls are shown as solid-coloured and quartered targets respectively. Typically, both are out of the y-z plane in question. The CG's of both hulls are always restrained in the x-z plane but they are not always on the centerline of a 2d section because the 3d hull is trimming.

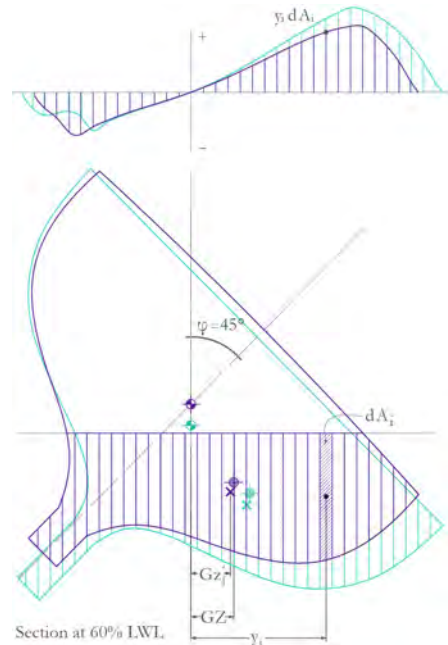


Figure 20 – Transverse sections of two hulls with the submerged planes cut into vertical strips.

The moment of the area of a vertical elemental area below the waterline (dA_i) about the x-axis is:

$$M_{A_i} = y_i dA_i \quad (1)$$

In the *Open Sea* routine, *Grasshopper* plots the values of the moment of area of each elemental area as ordinates on the graph above, and then fairs a curve through them. These curves represent the moment contributions of elemental prisms of volume across the transverse section to the global righting moment (and the sum of $y dA$ across the section is the first moment of inertia).

If we consider superimposed transverse sections of two hulls at the same relative point along their hulls, we can compare the transverse distribution of volume in the two hulls at that particular relative station by direct inspection. If we also superimpose the curves of $y dA$ on top of each other, we can compare the relative contributions to local righting moments of discrete volumes across the two transverse sections. These can change significantly along the length of the hull, as can be seen in Figure 21, which reveals a significant difference in the behavior of the two hulls.

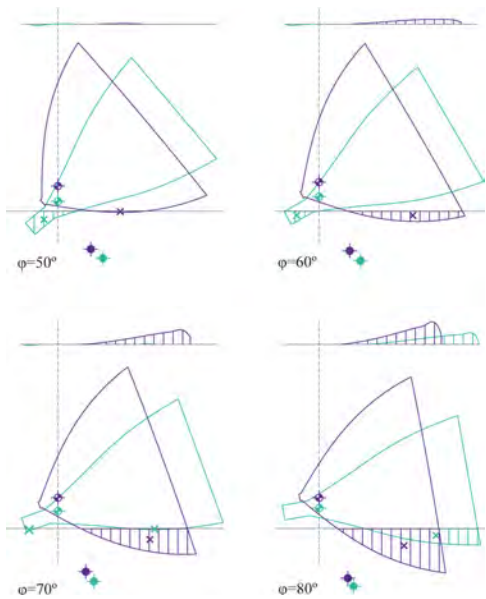


Figure 21 – Comparison of sections at 5% of LWL

We can also look at the distribution of righting moment longitudinally. Figure 22 shows the shape of the water planes as the hulls heel over. The concave edge at the bottom of the water planes is the curved surface (sheer) of the deck as it is submerging. The small projection at the top left is the back end of the skeg. The centres of buoyancy are shown, and the dashed longitudinal curves run through each local sectional centroid (X's in Figure 20), giving a useful indication of how the local righting arms (Gz_j) of each section vary along the length of the hulls at that angle of heel.

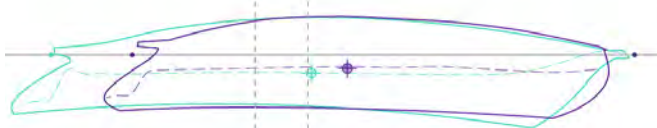


Figure 22 – Water planes of the heeled hulls

We can plot the full series of ydA curves from each station down the length of the hull, in 3 dimensions. These curves can be seen within the coloured surface in Figure 23. The *Open Sea* script lofts a surface over the curves and conditionally colours it based on the amplitude of ydA at any given point. This colour map shows the distribution of righting moment over the entire water plane at any given angle of heel. Red and yellow show areas of high local righting moment, while blue areas show high local overturning moment.

Figures 21 and 22 further explain the shallow slope of 'VA's' GZ curve: Figure 21 shows that through an arc from 50° to 70° at sections 5% aft of the origin, 'VA' is producing positive righting moment from volume in the bows, while at the same station in #4f, only contrary overturning moment is produced from the immersed volume. The difference can clearly be seen in the diverging dashed lines in the bows in Figure 22.

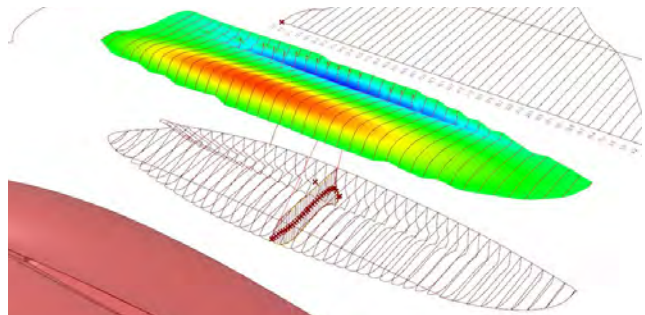


Figure 23 – Distribution of righting moment

Further discussion of the *Open Sea* analysis and the GZ curve of the 'VA' hull is beyond the scope of this paper. The analysis did have a significant impact on the evolution of the hull form of the new schooner. In essence, the issue is simple: maximize the buoyant righting volume that can be engaged as the hull heels, and minimize the amount of counterproductive volume below the waterline.

The outcome of our analysis and stability-related design efforts will be parsed in more detail in a future paper, but is summarized in Figures 24 and 25. Figure 24 shows a robust GZ curve for recent hull iteration DS067 with a plausible VCG of -0.38m, along with the MCA wind heeling arms and a tabulated assessment of compliance with Transport Canada Marine Safety regulatory requirements. The area under the curve to 90 degrees is 34% greater than the area under #4f's curve (shown as a light dotted curve)—a non-trivial difference. Areas from 0° – 30°, 0° – 40°, and 30° – 40° exceed Transport Canada and IMO intact stability requirements by ~370% – 450%. The angle of intersection between the GZ and gust heeling arm ($HAgust$) curves is large. The calculated steady angle of heel is greater than 31 degrees, approximately 10 degrees beyond the angle of deck edge immersion and the normal operational limit of heel. GZ_{max} is almost 1m at ~44 degrees, and from GZ_{max} to 90 degrees, GZ for the bare hull drops by 26% (cf. 61% for #4f). At 85 degrees, GZ for the hull plus preliminary deck structures has dropped by only 9%.

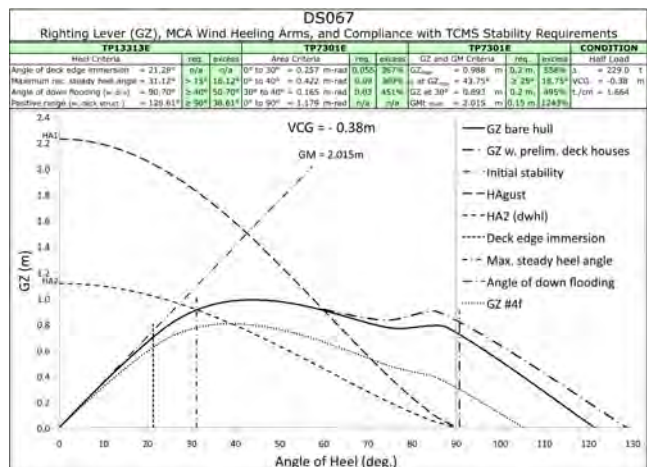


Figure 24 – GZ of DS067 with MCA criteria and tabulated Transport Canada Marine Safety requirements

In Figure 25, the dashed blue lines at the top are the righting moment curves of DS067 for two projected heights of VCG. The lighter curves that appear above them at 60° show the difference made when the (preliminary) deck structures start to submerge. These curves show that the DS067 hull has more than double the righting moment exhibited by #4f (solid black curve) in knockdown condition, but it should be noted that much of the difference is due to a significant drop in VCG caused by the addition of a very large (>65 tonne) ballast keel.

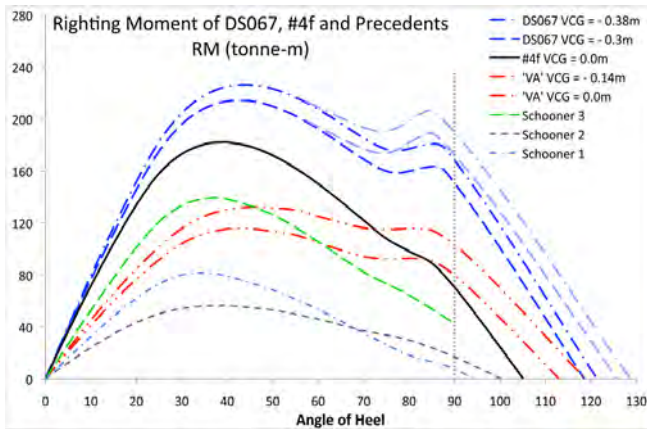


Figure 25 – RM of #4f, DS067 and precedents

While the first part of the descending dashed blue curves look parallel to the curve of #4f, it must be remembered that they reflect the significant counterproductive volume of the ballast keel itself—without that volume, GZ would increase significantly and the bump of the emerging keel would largely disappear.

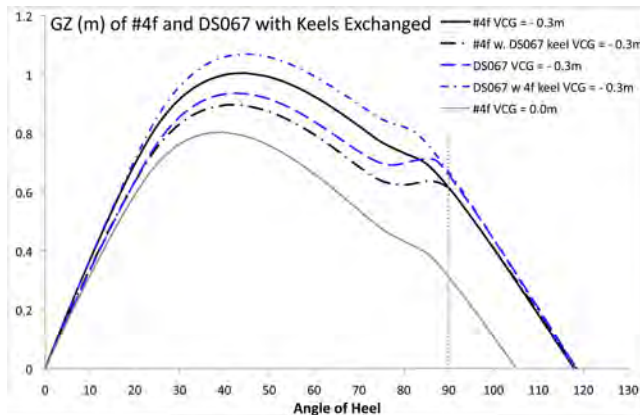


Figure 26 – GZ of #4f & DS067 with keels exchanged

This effect can be examined by exchanging the keels on the two models and matching their VCG's, as shown in Figure 26. The solid black curve shows GZ for #4f with a VCG of -0.3m (GZ for VCG of 0.0m, as seen in earlier figures, is shown as a grey line). A VCG of -0.3m is not physically achievable in the #4f hull, however, and can only be realized with the addition of a deeper ballast keel. The black dash-dot curve shows the detrimental effect of

adding the DS067 keel to the #4f hull. Conversely, the blue short dash-dot curve shows the increase in GZ that results from reducing the volume of DS067's keel by replacing it with the keel from #4f. The difference between the curves for DS067 and #4f with the larger keel elucidates the effect of the form differences between the two canoe bodies.

Downflooding and Capsized Flotation Plane

With the heightened risks associated with carrying sail, we deemed it imperative that all operable deck openings be located on the centerline (this is consistent with best practice). In both the *Pride of Baltimore* and *Concordia* casualties, downflooding occurred through offset hatches or doors.

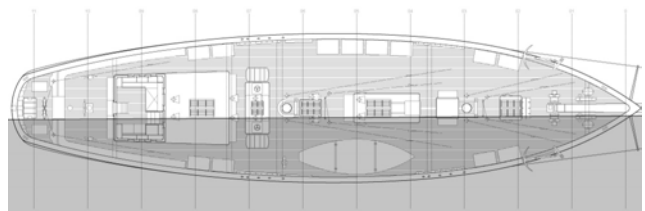


Figure 27 – Intact flotation line with the vessel on its beam-ends at 90 degrees heel.

Assuming a complete 90° knockdown is possible, we have paid attention to how deck openings relate to the capsized flotation line. As can be seen in Figure 27, the vessel has sufficient buoyant volume to float on its beam-ends with all centerline openings clear of the water. This was an explicit design objective.

CODE COMPLIANCE

As a condition for certifying the new schooner for unlimited international voyages, Transport Canada is requiring that SALTs design the boat to meet the standards of the IMO *Code of Safety for Special Purpose Ships* (SPS). If SALTs' new schooner is successfully built to meet this code, it will be the first SPS-certified sail-training vessel in Canada, and may be—we are not certain but would like to know—the first wooden SPS sail-training boat in the world.

While the SPS code explicitly applies to sail-training vessels and considers trainees to be special personnel—neither passengers nor crew—significant code-compliance issues have been encountered, stemming largely from the size of the boat and the materials of construction.

The SPS Code was developed for new ships of 500 gross tonnage and above, and it refers broadly and significantly to SOLAS, in which the standing assumption is that vessels are made of steel. For the most part, for an SPS vessel of this size and complement (~156 GT and 45 crew and trainees), SOLAS standards for cargo vessels apply. Notwithstanding the SOLAS provision for alternative design and arrangements, certain requirements cannot be met, and meeting others will be arduous and expensive.

For instance, the inclination of stairways may not exceed 50 degrees. In a vessel of this size, the longitudinal traverse of stairs at that angle would use up so much space below that key uses would be badly compromised or knocked out altogether. The length of the deck-head opening would have to be increased to the point where closure would be unmanageable, and its size would be in direct conflict with the imperative to reduce the risk of downflooding. Citing these conflicts, non-SPS precedents, and SALTS' 35-year record of safe operation, our strategy will be to propose an engineered ladder with climbable sides that provide lateral restraint when the ladder is climbed on the principal rungs.

The SOLAS requirement for a 760mm deep double bottom is not consistent with the size of the vessel or traditional wooden construction. In response, we are considering a probabilistically-based proposal to relax the related SOLAS rule regarding longitudinal extent of damage, based on bottom protection afforded by the keel.

Structural fire protection is perhaps the most challenging—and certainly the most expensive—regulatory requirement we must address. SOLAS-compliant precedents and the excellent fire performance of heavy timber construction form the foundation of our proposal, along with enhanced fire safety measures including interior steel bulkheads, subdivision of machinery spaces, elimination of non-essential heat sources, extensive use of intumescent coatings, additional fire insulation, a high-pressure fog fire suppression system, and increased redundancy and separation of fixed fire pumping capabilities.

SPS compliance is complex and figures significantly in the design of this boat. Further discussion of the issues and design responses will be presented in a future publication.

DESIGN DEVELOPMENT

Integrated Design Process

At the onset of the first phase of design development, we had a fairly comprehensive but still evolving understanding of the complex web of design criteria that needed to be addressed. To the degree that was possible, our goal was to proceed with a fully integrated design process. The story of the detailed development of the current design is complex and too long to address here. Although it is the heart of the issue, what follows is merely a synopsis.

Hull form

With the work we had done in preliminary design converging on a fit between the GA and the hull envelope, we began the process of defining a new baseline hull. We had established parametric design targets and a target curve of areas based on our analysis of precedents, the literature, and the advice of consultants.

Rather than continuing to adjust the existing surface in the #4 series of models, we started from scratch, generated a new hull surface, and then proceeded to develop it in a fully integrated fashion, with cyclical attention paid to hull aesthetics, the spatial requirements of the GA, safety, stability, hydrodynamics and parametric targets, the

position and design of the rig and the question of balance, regulatory requirements, and hull structure.

The evolving hull envelope departed significantly from the #4 series, with a more gracefully curving stem, a longer counter that anticipated a transom, a flatter run of buttocks, and less deadrise. The rocker keel was introduced about a third of the way through the baseline series (BL), inspired by William Gardner's famous schooner *Atlantic* (1903) and the lines of the pilot schooner *America* (1897), designed by Thomas McManus (Cunliffe 2001). The basis for this decision was a hypothesis that the curvature would relate to flow trajectories and have general hydrodynamic benefits, and the fact that the point of greatest draft would occur where the ballast keel was widest, thus lowering VCG.

Our workflow shifted between traditional and digital media. Pencil was integrated with digital drawings and models. We cut a series of wooden half models using a CNC router at the University of Oregon so that we could inspect a physical hull surface visually and feel it in our hands. The use of *Grasshopper* circumvented the limitations of stock programs and empowered design—we have yet to imagine a modeling or analysis task that we could not accomplish. It took only the addition of a fairly simple script to our standing *Open Sea* algorithm for hydrostatics to allow us to look at the shape of the heeled waterlines of evolving hull prototypes—something we attended to carefully as we refined the lines (Figure 28).



Figure 28 – Waterlines of hull BL049 at 20° heel

The baseline series of hull surfaces ran through sixty-five iterations, until we reached what we deemed the definitive baseline hull for the pending experimental campaigns (Figures 29 - 30). Aesthetically, however, the hull was not yet resolved above the waterline, particularly the sheer and the form of the stern and transom.

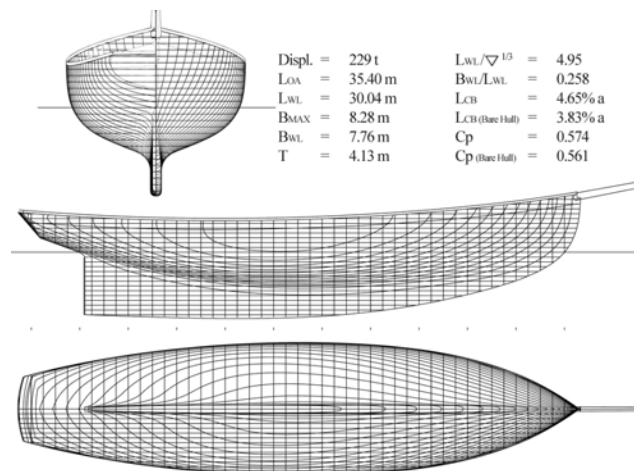


Figure 29 – Lines plan of prototype BL065

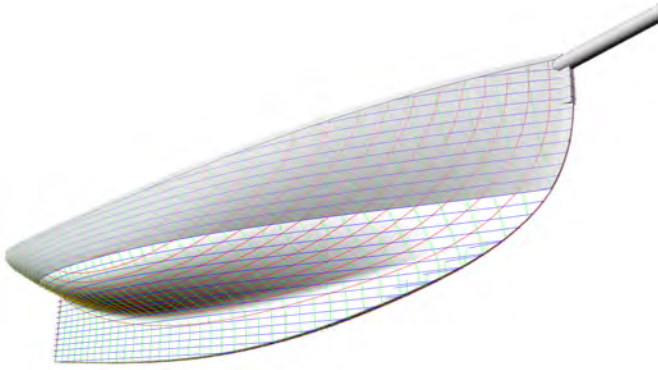


Figure 30 – Perspective view of BL065. Note the rocker keel and relatively flat deadrise midships.

Mockups and 3d Models

Concurrent with the hull work, development of the GA proceeded with drawings, detailed 3d models in *Rhino* (Figures 31 – 32) and, unusually, a full-scale cardboard mockup of the aft cabin space built by students to definitively confirm that its size and proportions were correct.

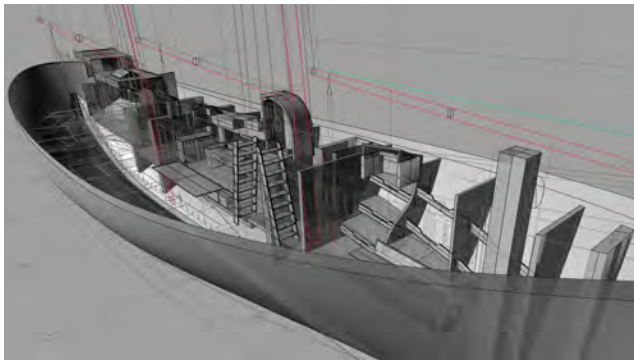


Figure 31 – Early 3d model of the GA below

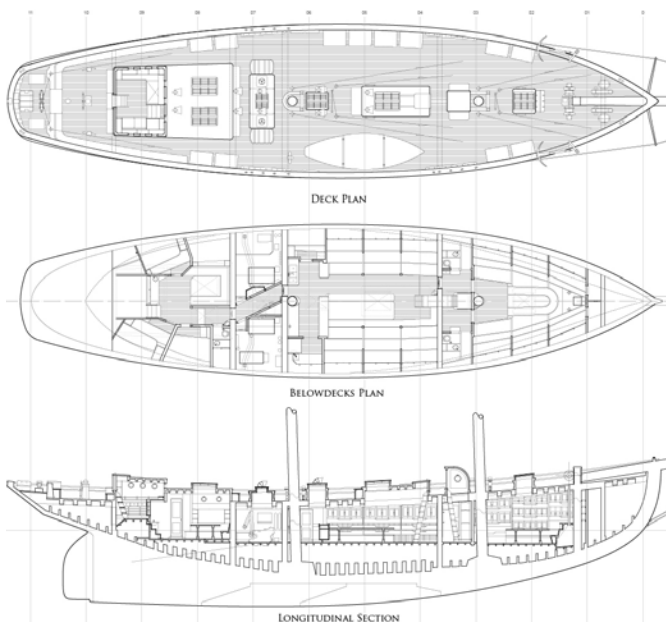


Figure 32 – General arrangement as of August 2012

Hull Structure and Mechanical Systems

We have not started detailed engineering and construction drawings, but we have worked through a preliminary definition of the wood hull structure (Figures 33 – 34). We expect that the vessel will be built to rules and scantlings extrapolated from Lloyds Registers' *Rules and Regulations for the Classification of Small Craft*, with a laminated backbone, continuous laminated frames midships, (possibly) laminated beam shelves and lining, and carvel planking.

Principal engineering concerns that we are now addressing are general hull strength, stiffness and long term deformation (hogging is a significant concern); finding an appropriate balance between building for strength and stiffness and building for ease of long term repair; dealing with high predicted rig forces in wood masts and hull structure (we must design for maximum righting moment plus a factor of safety); and ballast keel attachment.



Figure 33 – *Rhino* model of primary hull structure

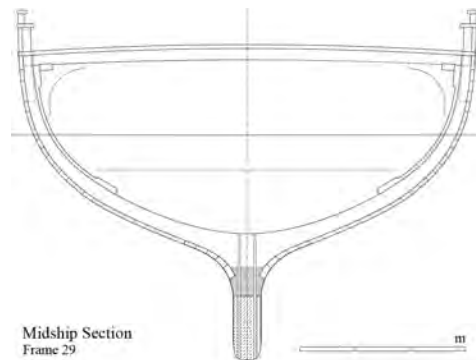


Figure 34 – Continuous frames above keel

TOWING TANK CAMPAIGN

Test Program and Procedure

The first experimental investigation was a three-day towing tank campaign conducted at the Wolfson Unit at the University of Southampton, England. Campaign objectives included a qualitative assessment hull performance, visualization of flow trajectories to determine the depth that water is deflected by the canoe body, evaluation of upright hull resistance to determine powering requirements, quantification of the effect of changes in keel draft and profile on resistance and side force, evaluation of the position of CLR in response to changes in keel profile, side force, and rudder angle; and assessment of the implications of changes to the keel profile on helm balance and stability.

A 1:15 scale model of the hull and three interchangeable keels were built by SALTS (Figures 35 - 36). The 60m x 3.8m x 1.8m towing tank at Southampton Solent University was used. The model was towed using a dynamometer that allowed the model freedom to heave and pitch, but provided restraint in yaw, sway and roll. For upright tests, the model was ballasted to float on the design waterline. For tests in the sailing condition, ballast was shifted to heel the boat and eliminate static restraint roll moments, a trim moment was applied to correct for the point of tow, and weights were added to simulate the downward thrust of the sails.

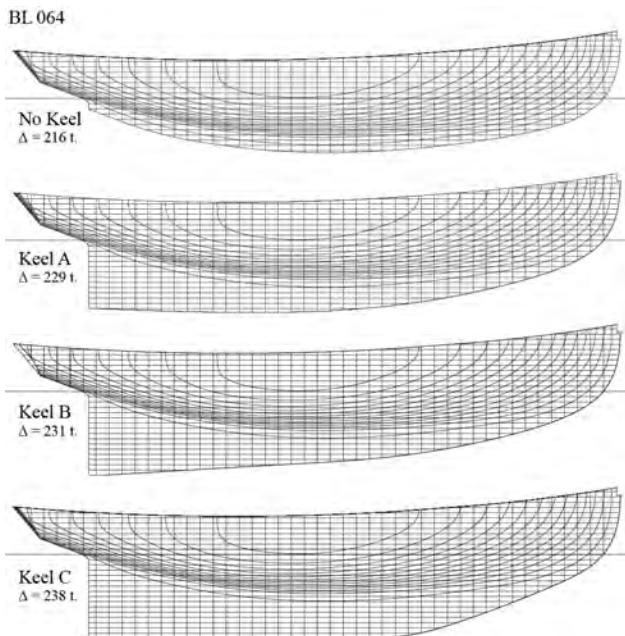


Figure 35 – Canoe body and test keel profiles

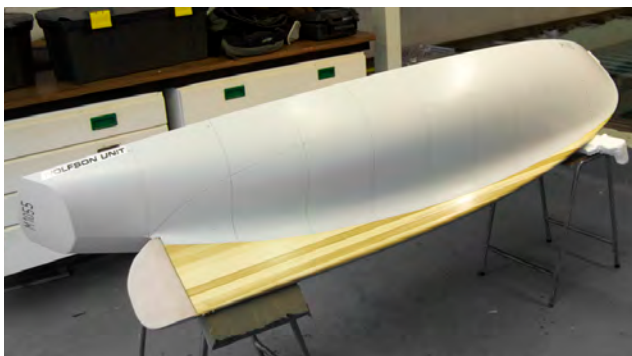


Figure 36 – Tank model with Keel A and rudder

For upright tests, resistance, trim and heave were measured. For tests with restrained angles of heel and yaw, resistance, side force, and yaw and roll moments were measured. To ensure consistent model boundary layer conditions, the hull was fitted with turbulence-inducing studs, and resistance data were corrected to allow for the resistance of the studs and the region of laminar flow ahead of them.

The corrected model resistance data were extrapolated to full scale using a modified version of the ITTC Model-Ship Correlation Line to calculate the skin friction resistance. No allowance was made for any region of laminar flow on the full-scale craft. The total skin friction resistance was calculated from the total wetted surface area of hull keel and rudder, with Reynolds Numbers calculated based on the hull waterline length.

The three keel configurations and the bare canoe body were tested in the upright condition at full-scale speeds ranging from 5 to 16 knots. Heeled and yawed tests were conducted with the three keel configurations across a test matrix of varied speed, heel, yaw and rudder angles.

Preliminary Results

Observations of the tests and inspection of photographs (Figures 37 - 38) showed that the model ran extremely well, with a single well-defined symmetrical midship wave trough, minimal breaking of the bow wave, and no evidence of wake thickening before the transom was reached, except at the highest speeds.



Figure 37 – 11 knots ($F_n = 0.33$) upright



Figure 38 – 12 knots ($F_n = 0.36$) 15° heel

Figure 39 shows the variation of trim and heave with speed. At 13 knots ($F_n = 0.39$), bow up trim was less than 0.4 degrees—satisfactory for a sailing vessel with such a high displacement to length ratio.

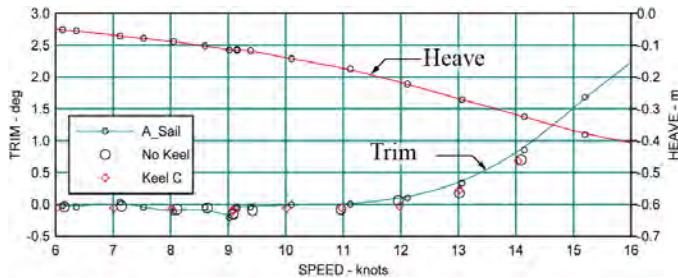


Figure 39 – Variation of trim and heave with speed

To evaluate the effect of keel volume on resistance, the residuary resistance coefficient (C_{rr}) was calculated, as given by:

$$C_{rr} = \frac{R_r \cdot 1000}{\Delta \cdot F_n^2} \quad (2)$$

The variation of C_{rr} with speed showed that the bare hull with no keel had the highest specific residuary resistance, despite having the lowest displacement (Figure 40). The larger the keel volume, the lower the C_{rr} , indicating that volume can be carried in the keel relatively cheaply, because it is more deeply immersed and therefore creates less energetic surface waves.

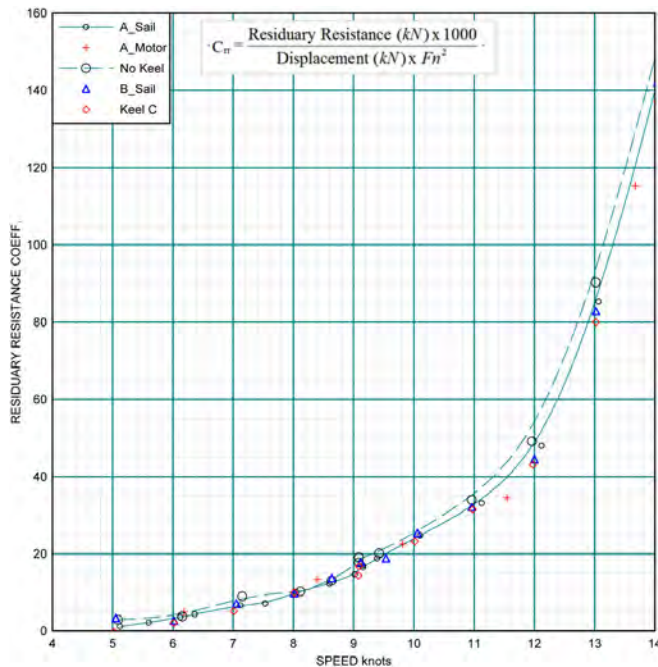


Figure 40 – Residuary resistance coefficient

Oil-flow visualization showed that the flow direction over the hull aligned quite closely with the cut line at the

top of the keels (see Figure 36). The rising trajectory of flow in the stern (Figure 41) suggests that a modest rise in keel profile towards the stern would be well matched to local flow.



Figure 41 – Oil streak flow visualization; Keel C

Figure 42 shows the ratio of resistance of keel configurations B and C and the bare hull to Keel A, all at zero heel. Deepening the keel increases wetted surface area and hence viscous resistance, but the relative effect is seen to diminish with speed as residuary resistance increases.

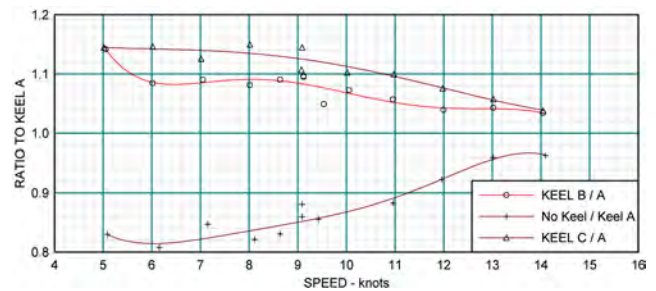


Figure 42 – Resistance ratio to Keel A (upright)

When the vessel is heeled, the deeper keels can recover this drag deficit and more, however, because the deeper keels create side force more efficiently. In general, resistance data for each speed and heel angle plotted against side force squared collapse to straight-lines, and it is therefore possible to ascribe an effective aspect ratio and, correspondingly, an effective draft (T_{eff}) to the hull-keel combinations, as given by:

$$T_{eff} = \sqrt{\frac{1}{(dR/dSF^2) \cdot \rho_w \cdot \pi \cdot V^2 \cdot \cos^2 \varphi}} \quad (3)$$

The slope of the plotted lines is a measure of how efficiently the hull, keel and rudder produce side force in terms of induced drag penalty (Claughton, Wellicome and Shenoi 1998).

Figure 43 shows resistance and CLR position vs. side force squared for the three keels tested at 10 knots and 10

degrees of heel, at yaw angles ranging from 1 to 6 degrees. As can be seen in the upper part of the figure, when side force is low, Keel A has the lowest resistance; but as side force increases and at higher heel angles (tested but not shown here), the deeper keels exhibit the lowest resistance. To interpret this result meaningfully, the designer must know the equilibrium side force value for the heel angle under consideration. For this vessel the equilibrium side force² at 10 degrees of heel is approximately 2500 kN². Thus the extra drag of the deeper keel does not net out to a lower drag. As heel angle increases, however, the equilibrium side force increases, and the deeper Keel C gives the lowest resistance.

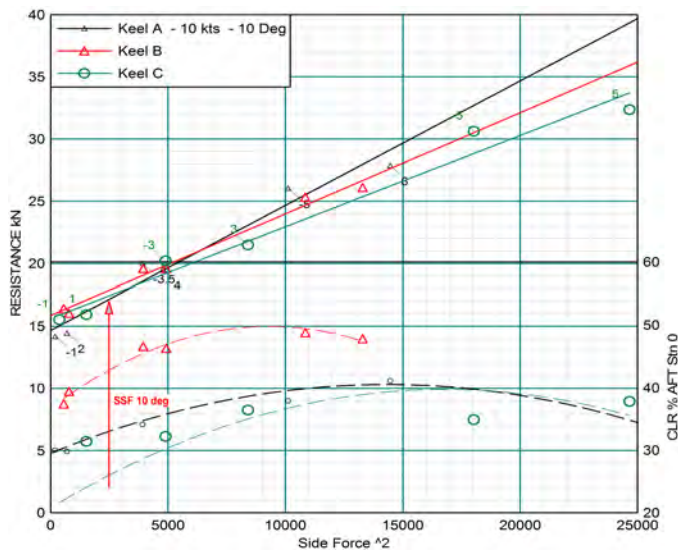


Figure 43 – Resistance and CLR position vs. side force squared for keels A, B and C at 10° heel

Position of the Centre of Lateral Resistance

The longitudinal positions of CLR can be obtained by dividing the measured yaw moments by side force, and these can also be plotted against SF², as shown in the lower part of Figure 43 (and graphically in Figure 59). These results, for 10° heel, and at higher angles (not shown) clearly show the difference in the position of CLR for Keel B compared to Keels A and C.

While only partial results have been presented in this paper, the data gathered in the towing tank campaign illustrate the effects of changing keel profile and draft in full-keel displacement hulls. A final keel profile will be tested in the towing tank, and these results will be combined in the WinDesign6 VPP (Claughton & Oliver 2003) to develop polar curves and sail selection charts, informed by a yaw moment equilibrium calculation to check the sailing rudder angles (Claughton 2012).

WIND TUNNEL CAMPAIGN

The second experimental investigation was conducted in the twisted flow boundary layer wind tunnel at Politecnico di Milano, Italy. A peculiarity of the facility is the presence of two test sections of very different characteristics,

offering a very wide spectrum of flow conditions, from very low turbulence and high speed in the contracted 4 x 4m section ($Iu < 0.15\%$, $V_{max} = 55$ m/s), to earth boundary layer simulation in the large wind engineering test section. As shown in Figure 44, the P.d.M. wind tunnel is a closed circuit, with the two test sections arranged vertically and airflow generated by an array of 14 axial fans.

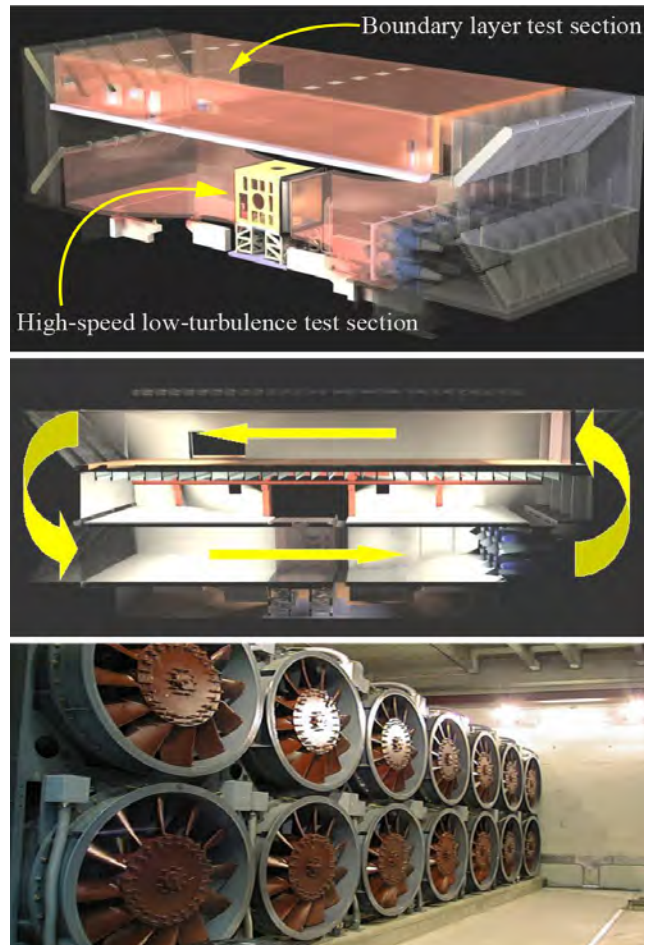


Figure 44 – Politecnico di Milano Wind Tunnel

The large 36m x 14m x 4m size of the boundary layer test section used for this investigation facilitates very large-scale wind engineering simulations: for aerodynamic studies of yacht sails, it enables the testing of large scale models (typically 1:10 - 1:12 for IACC yacht models) with low blockage effects at a maximum speed of 15 m/s. A twisted flow gradient can be created, reproducing both the increase in incident apparent wind speed and the rotation of apparent wind direction away from a yacht's heading that are experienced in real life with increased height.

Test Apparatus, Program, and Procedure

A complete working schooner model was mounted on a six-component dynamometric balance fitted in the wind tunnel's 13m-diameter turntable (Figure 45). The large size of the low-speed test section permits the use of quite large yacht models. Sails are therefore large enough to be made

using normal sail making techniques, the model can be rigged using standard model yacht fittings, and most importantly, deck layout can be reproduced around the sheet winches, allowing all the sails to be trimmed as in real life.



Figure 45 – Model with sail plan S5 at 60° AWA

SALTS built a 1:15 scale model at their shipyard in Canada, closely matching details of the boat's design and the technology of the rig. A rigid aluminum chassis served as the foundation for the entire model. Mast steps, deck structures, rig fittings, travelers, and servos were mounted directly on the chassis. A fiberglass yacht hull body was suspended off the chassis, 3 mm clear of the turntable, and a curved cardboard surface was fitted to simulate design deck sheer (Figure 46). The standing rig was built with correctly tapered masts and spars, wire shrouds and stays, and simulated ironwork (Figure 47). Model sails were designed and built by Doyle Sailmakers.



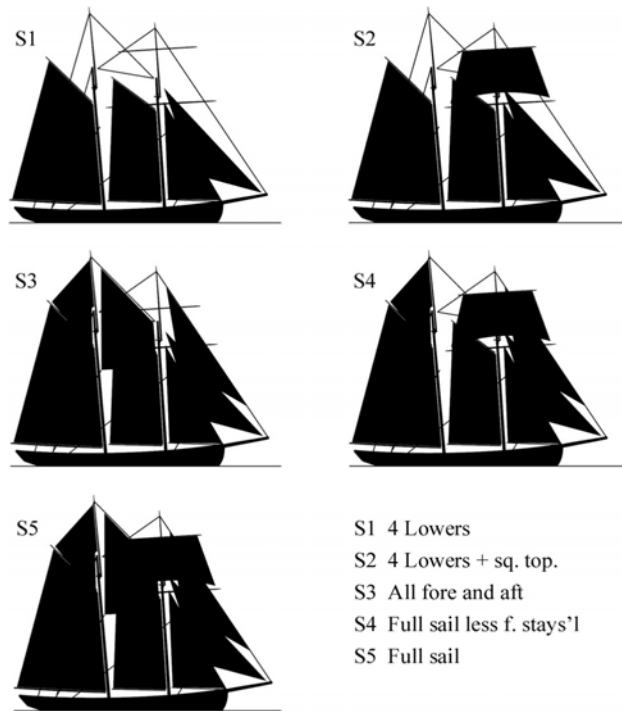
Figure 46 – Deck layout

Over the course of a five-day wind tunnel campaign, fifteen sail plans were tested—five principal suits of sails (Figure 48), followed by ten variations of important sail plan geometries: mast rake, mainsail size, and headsail size and position. Campaign objectives included a detailed

investigation of the aerodynamics of a traditional square topsail schooner rig, and the provision of data useful for design development in terms of balance assessment and performance prediction.



Figure 47 – Detail of the standing rig.



- S1 4 Lovers
- S2 4 Lovers + sq. top.
- S3 All fore and aft
- S4 Full sail less f. stays'l
- S5 Full sail

Figure 48 – The five principal suits of sails tested

Models were tested in the upright condition at six fixed apparent wind angles from 30° to 150°, under constant dynamic pressure (Figure 49). Windage tests were performed on the bare hull and rigging at apparent wind angles from 0° to 180°.

Sails were trimmed to achieve maximum driving force by monitoring real-time force data while observing the sails directly from the control booth and using live video-feed

from three cameras positioned in the wind tunnel. The sails were then depowered according to a consistent scheme, with data recorded in steps, as heeling force was reduced to approximately 50% of observed maxima. At each trim condition, 30 seconds of data were recorded at 100Hz sample frequency. Time histories and mean values for all measured quantities were stored in a file, and subsequently corrected for residual zeroes error due to temperature effects.



Figure 49 – S2 at 90° AWA and S3 at 40° AWA

Data Analysis

The usual way of analyzing wind tunnel data is to compare non-dimensional coefficients, enabling comparison of the efficiency of sail plans of different total area at different conditions of dynamic pressure. The first analysis performed was the variation of non-dimensional driving (C_x) with heeling (C_y) force coefficients, as given by:

$$C_x = \frac{F_x}{\frac{1}{2} \rho_a S v^2} \quad (4)$$

$$C_y = \frac{F_y}{\frac{1}{2} \rho_a S v^2}$$

Figure 50 shows a comparative plot of C_x vs. C_y for sail plan S4 (see Figure 48 and frontispiece) at four of the apparent wind angles tested. Each run at each AWA is plotted as an independent data point. It can be seen that there are some settings at the highest values of heeling force coefficients where the driving force is lower than the maximum value. These non-optimum values were obtained by over-sheeting the sails, such that the mainsails generally had a tight leech and the airflow separated in the head of the sails. After maximizing the driving force, the sails were adjusted to reduce the heeling force, initially without reducing the driving force. In Figure 50, envelope curves have been drawn through the test points with the greatest driving force at a given heeling force: data from non-optimal sail trim falling below the envelope curves are excluded from the subsequent analysis.

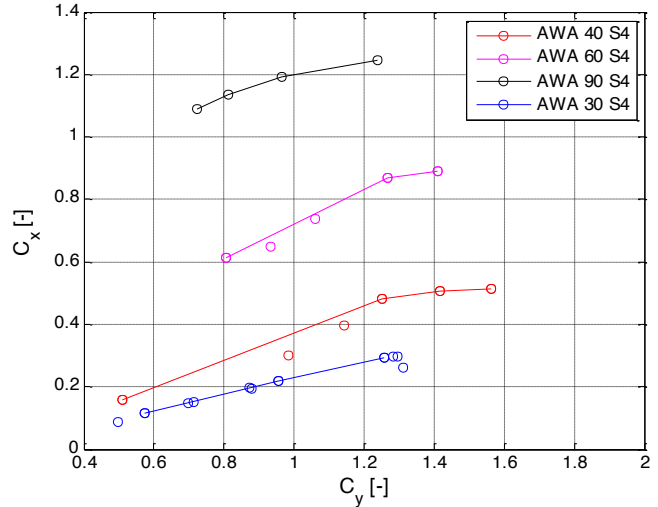


Figure 50 – Variation of C_x vs. C_y for sail plan S4

Heeling and yaw moments were measured and subsequently used to determine the center of effort positions of each sail plan tested.

The center of effort height, C_{eh} , is obtained by dividing the roll moment by the heeling force component in the yacht body reference system. A plot of center of effort height vs. heeling force for four apparent wind angles is shown in Figure 51. As can be seen, the center of effort

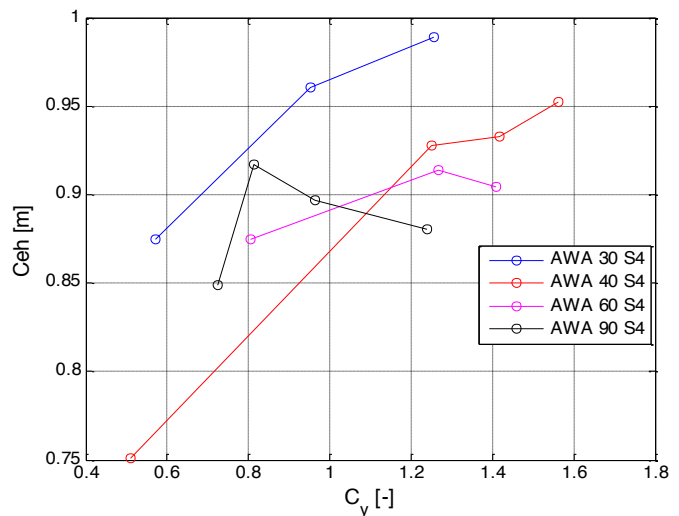


Figure 51 – Variation of C_{eh} for sail plan S4

height tends to reduce as the heeling force coefficients reduce. This is explained by the way in which the sails were depowered.

The center of effort longitudinal position, C_{ea} , is obtained by dividing the yaw moment by the heeling force component in the yacht body reference system. A plot of C_{ea} vs. heeling force for sail plan S4 at four apparent wind angles is shown in Figure 52.

More information can be extracted from the wind tunnel data by transforming them into lift and drag coefficients (Figure 53).

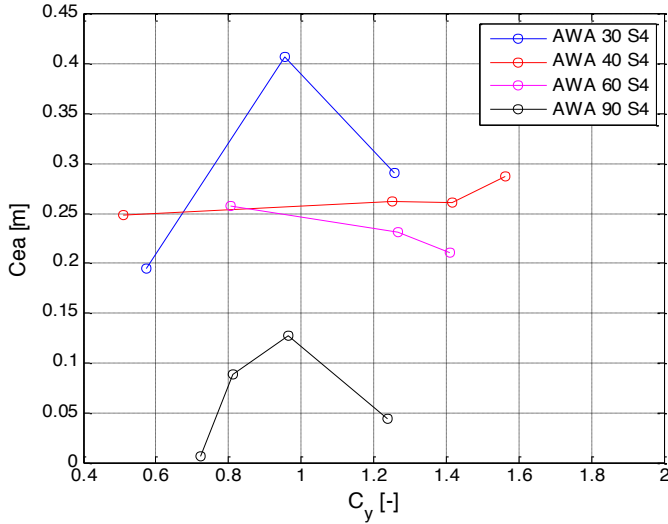


Figure 52 – Variation of C_{ea} for sail plan S4

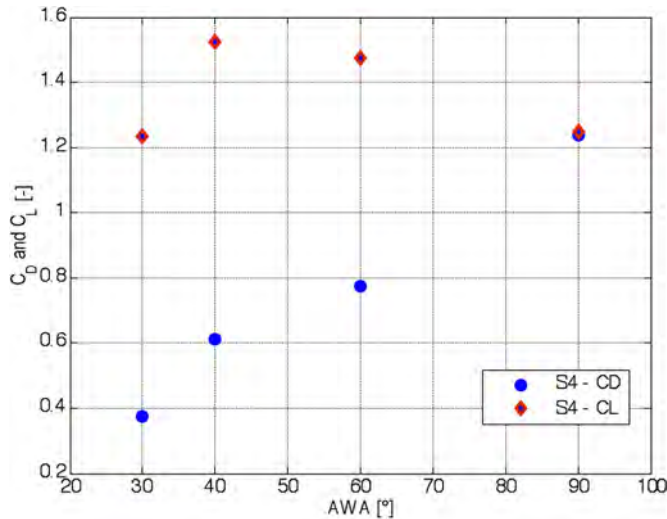


Figure 53 – Variation of C_D and C_L with AWA

Because both the induced drag and quadratic profile drag vary with the square of lift, it is informative to plot drag coefficient vs. the square of the lift coefficient as shown in Figure 54.

As can be seen, for reduced values of C_L , drag increases linearly, following a straight line. This linear increase is attributable to the induced drag. The effective height (H_{eff}) is a measure of the efficiency of the rig, and can be determined from the slope of the straight line by applying simple aerodynamic theory according to the following equation:

$$H_{eff} = \sqrt{\frac{SailArea}{\pi \cdot Slope}} \quad (5)$$

At higher values of C_L^2 , the values of C_D increase more rapidly with C_L^2 . This additional drag can be attributed to flow separation from the sails. Residual base drag—caused by viscous phenomena related to windage but not linked to

the production of lift by the sails—can be evaluated as the parasitic drag coefficient from the intercept with the zero lift axis of the straight line that runs through the test data at lower values of C_L^2 .

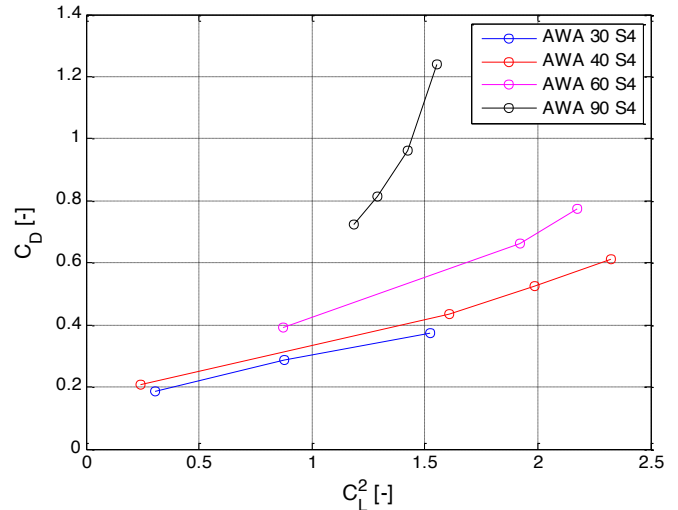


Figure 54 – Drag coefficient vs. lift coefficient²

Preliminary Results

In this paper, limited preliminary results are presented, anticipating the future publication of detailed results and additional work.

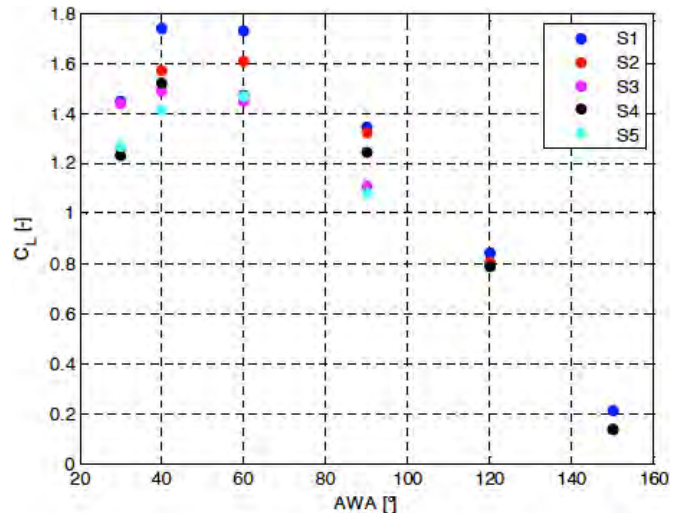


Figure 55 – Maximum lift coefficients C_L

Figures 55 and 56 show a comparison of the aerodynamic coefficients obtained from the five principal suits of sails (Figure 48) against the full range of apparent wind angles considered during the experiments.

Figure 57 shows the effective height values (at model scale) evaluated for each sail plan at the closest apparent wind angle tested (30°). As can be seen, the S1 configuration (four lowers) has the lowest efficiency. Efficiency increases as the number of individual sails in the upper part of the rig is increased and overall sail plan aspect ratios are higher.

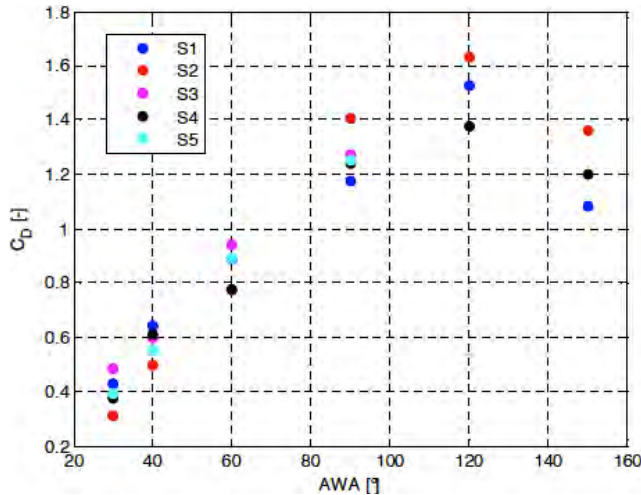


Figure 56 – Maximum drag coefficients C_D

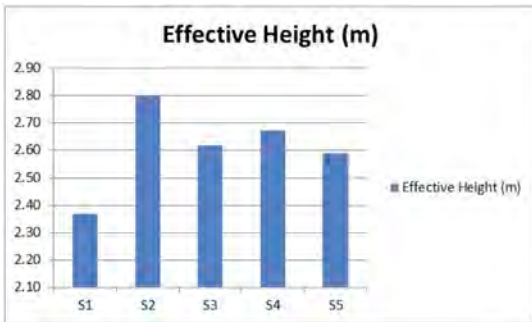


Figure 57 – Effective height values

These data, together with the center of effort positions for each sail plan, constitute the fundamental database for VPP analysis, which will be used in this project to inform further detailed design. When extrapolated to full scale, the experimental data will provide the necessary loadings for rig force analysis and subsequent rig structure design.

AERO-HYDRODYNAMICS AND BALANCE

Achieving good helm balance was the principal impetus for the towing tank and wind tunnel campaigns. In the early stages of design, the so-called *lead* of the geometric CE ahead of the geometric CLR was considered, but it was clearly understood that this has no direct relationship to real physics. In particular, since the design of the schooner was not following an historical or current precedent and the geometry of the sail plan and keel profile differed from sailing vessels we knew well, lead was considered to have only limited usefulness.

It is interesting to note, however, the differences between the geometric and aero-hydrodynamic data. The aerodynamic centres for all five principal sail plans are located lower and forward of the geometric centres, as illustrated in Figure 58, with a mean difference in longitudinal position of 8.4% of LWL.

The differences between the geometric and hydrodynamic CLR's are much greater, as shown in Figure 59, in which geometric centroids are plotted as quartered targets

and test results are shown as shaded zones that correspond to the range of the location of the CLR as it varied with sailing side force. The delta between geometric centroids and experimental CLR's ranged from 17% (Keel B) to 34% (Keel C) of LWL. Moreover, the geometric and hydrodynamic centres of Keel C actually move in *opposite* directions away from those of Keel A.

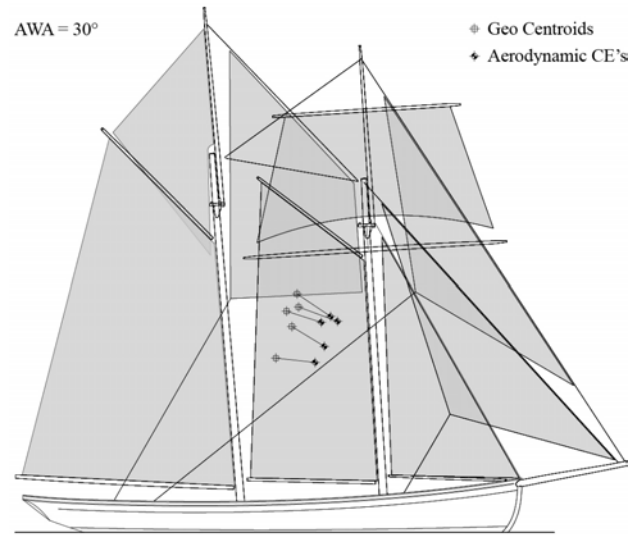


Figure 58 – Geometric and aerodynamic centres

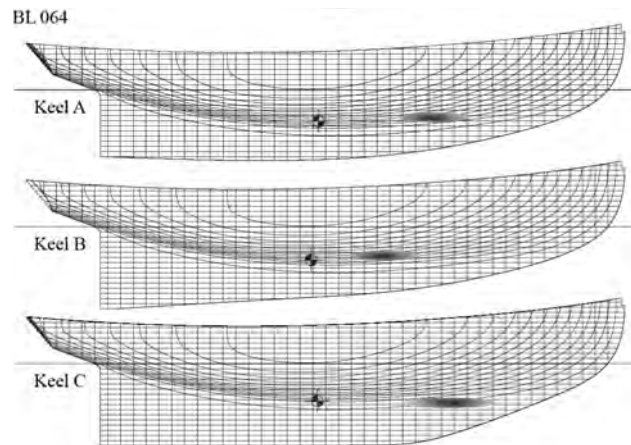


Figure 59 – Geometric and hydrodynamic CLR's

Analysis of the data from the two campaigns suggest that the CLR of the design keel (A) is too far forward: for sail plan S1, depending on the side force, rudder angles of 6.5° – 8.0° would be required to balance the boat. To achieve good helm balance, only Keel B has a CLR sufficiently far aft to maintain an acceptably low rudder angle. As its draft exceeds SALTS' design criteria in terms of accessibility to shoal waters, an alternate keel profile is being designed.

The limitations of the geometric rule-of-thumb approach are confirmed by the experimental results themselves. Throughout the design process, SALTS' larger schooner, the *Pacific Grace*, has been used as a principal design comparator. That boat is similar in size to the new design

convenient way of capturing good practice; it offers neither guidance for vessels that differ from the precedent ship, nor any information as to the consequences of missing the lead target. Only the adoption of a more sophisticated view of the interactions between righting moment, heeling arms and the resistance to side force ratio can do this. Recognizing that many future sail-training projects will not have the benefit of data obtained from towing tank and wind tunnel campaigns, the data presented here and in subsequent papers can be used by designers to take a more rational approach. Additional work may lead to useful guidelines for design.

To a degree, with its deep keel and higher-aspect rig, the design of the schooner itself departs from the canons of design often employed in the construction of replicas and interpretations of historical vessels built for sail training. The boat will clearly not be a replica of a North Sea Pilot Schooner. First and foremost, the boat is being designed to take young people to sea as safely as possible. Considered together, the anticipated improvements in safety, stability, and other aspects of design might prove to be a step forward in the evolution of sail-training vessels of this class.

ACKNOWLEDGEMENTS

The authors would like to thank Paul Gartside, Philip Thiel, Philip Langrish, Bill Curry, Sugar Flanagan, and Andy Davis for their generous advice. We thank Marytn Prince at the Wolfson Unit, and Politecnico di Milano wind tunnel staff Luca Ronchi, Sara Muggiasca, and Paolo Schito for their expert assistance. More than 40 students at the University of Oregon have participated in the project and to them, we express our gratitude, particularly to Kate Laue. We recognize the support of SALTS, the University of Oregon, the University of Southampton, and Politecnico di Milano. We thank Creative Systems, Inc. and CD-adapco for their generous donations of software, and the Woodland Trade Company for their extraordinary support and assistance.

ENDNOTE

A key aspect of the MCA stability criteria, based on the work of Barry Deakin at the Wolfson Unit, is the derivation of a ‘maximum recommended steady heel angle,’ beyond which a sailing vessel becomes vulnerable to downflooding in the event of a severe gust.

Quoting from the Transport Canada standard for sail training vessels, TP13313E, the derivation of the steady heel angle and associated heeling arm curves is as follows:

$$HA_1 = \frac{GZ_f}{\cos^{1.3} \varphi_f}$$

Where:

HA_1 = The magnitude of the actual wind heeling lever at 0 degrees which would cause the vessel to heel to the downflooding angle (φ_f) or 60 degrees whichever is least. [HA_1 is more commonly known as WL_0 .]

GZ_f = The lever of the vessel’s GZ curve at the downflooding angle or 60 degrees whichever is least.

HA_2 = The mean wind heeling arm at any angle φ degrees [HA_2 is more commonly known as the derived wind heeling lever, ‘dwhl.’]
 $= 0.5 \times HA_1 \times \cos^{1.3} \varphi$

In Figure 3, the heeling arm curve that follows from HA_1 is labeled as HA_{gust} . The maximum recommended steady heel angle is found at the intersection of the GZ and HA_2 curves (see Figure 24).

The logic of the MCA standard is that if a vessel is not sailed at an angle of heel greater than the derived maximum steady heel angle, it will not be vulnerable to downflooding in the event of a gust producing twice the mean wind pressure (a gust factor of 1.41). The likelihood of encountering a gust with a speed 41% higher than the hourly mean and of sufficient duration to cause serious downflooding is very low. The recommended maximum steady heel angle is independent of wind speed and the amount of sail area set, and thus can serve as a metric for the sailing master to judge a vessel’s safety in all conditions except sailing downwind. The greater the derived steady heel angle, the safer the vessel (Deakin 1991).

REFERENCES

- Claughton, A.R. (2012). ‘Hull sailplan balance, “lead” for the 21st century,’ 22nd International HISWA Symposium on Yacht Design and Construction, Amsterdam, 12-13 November, 2012.
- Claughton, A.R. and Oliver, J.C. (2003). ‘Developments in hydrodynamic force models for velocity prediction programs’, R.I.N.A. International Conference on The Modern Yacht, September, 2003.
- Claughton, Wellicome and Sheno, eds. (1998). *Sailing Yacht Design: Theory*, Chapter 14, Highfield, Southampton: University of Southampton ISBN 0-582-368567-X
- Cunliffe, T. (2001). *Pilots Vol. 1, Pilot Schooners of North America and Great Britain*, Brooklin, ME: Woodenboat, p. 135.
- Curry, B. (2010). ‘Report on the capsizing and loss of the *S.V. Concordia*, February 17, 2010,’ independently published.
- Deakin, B. (1991). ‘The development of stability standards for UK sailing vessels,’ RINA Journal, The Naval Architect, January 1991, pp. 1-20.
- Deakin, B. (2009). ‘Stability regulations of very large sailing yachts,’ 10th International Conference on Stability of Ships and Ocean Vehicles (STAB09), St. Petersburg, Russia, 22-26 June, 2009.

- Deakin, B. (2011). 'SALTS preliminary design review,' Professional communication.
- Fossati, F. (2009). *Aero-Hydrodynamics and the Performance of Sailing Yachts*, London: Adlard Coles Nautical ISBN 978-0-07-162910-2
- Fossati, F. et al. (2005). 'Twisted flow wind tunnel design for yacht aerodynamic studies,' Proceedings of the 4th European and African Conference on Wind Engineering, Prague, 11-15 July, 2005.
- Fossati, F. et al. (2006). 'Wind tunnel techniques for investigations and optimization of sailing yachts aerodynamics,' 2nd High Performance Yacht Design Conference, Auckland, 14-16 February, 2006.
- International Maritime Organization (2008). *Code of Safety for Special Purpose Ships*, London: International Maritime Organization.
- Parrott, D. (2004). *Tall Ships Down: The Last Voyages of the Pamir, Albatross, Marques, Pride of Baltimore, and Maria Asumpta*, New York: McGraw-Hill.
- Transport Canada (1999). *Standard Relating to Design, Construction and Operational Safety of Sail Training Vessels TP13313E*, Ottawa: Transport Canada Marine Safety.
- Transportation Safety Board of Canada (2011). 'Knock-down and capsizing – sail training yacht *Concordia* 300 miles SSE off Rio De Janeiro, Brazil 17 February 2010', Marine Investigation Report M10F0003, Ottawa: Minister of Public Works and Government Services Canada.